Supplementary material and methods.

Animal studies and diets. Lrh-1 liver specific knockout *(*LRH-1$^{-/-}$*) mice* were obtained by crossing mice with an Lrh-1 allele flanked by LoxP sites *(*Lrh-1$^{f/f}$*)* with albumin-Cre transgenic mice*.* Lrh-1$^{f/f}$ mice were provided by the Kliewer/Mangelsdorf lab and have been previously described (1)*; A*lbumin-Cre transgenic mice were provided by Bert O'Malley's laboratory at Baylor College of Medicine. Lrh-1$^{f/f}$ littermates served as wildtype (WT) controls. Methionine choline deficient diet (MCD, TD.90262) as well as the corresponding amino acid control diet (chow, TD.94149) containing 350g/kg choline dihydrogen citrate and 8.2g/kg methionine was custom made by Harlan Laboratories, Madison, WI, USA. 8-12 weeks old male WT and LRH-1$^{-/-}$ mice were fed either chow diet or MCD diet for 2 or 8 weeks (for measuring fibrosis) and harvested in deep anesthesia after isoflurane inhalation. Livers were excised, weighted and snap frozen in liquid nitrogen for further analysis or fixed in 4% neutral buffered formaldehyde solution and paraffin-embedded for light microscopy. Serum was collected by heart puncture at stored at -70°C until further analysis. Methods were approved by Baylor College of Medicine's Institutional Animal Care and Use Committee.

Cell Culture of AML-12 and C3HepG2 cells. Murine AML-12 and human C3A/HepG2 cells were kept in Dulbecco's modified Eagle's medium with nutrient mixture F-12 (DMEM/F-12; 113320; Invitrogen) or DMEM/F-12 media lacking methionine and choline (custom made DMEM/F12 MCD media, Invitrogen). Medium was changed every 24 hours. All experiments using cell lines were run in triplicates and reproduced at least in two independent experiments.

Serumbiochemistry. Alanine aminotransferase (ALT), aspartate aminotransferase (AST) and lactate dehydrogenase (LDH) serum levels were analyzed with a Hitachi 917 analyzer at the Center for comparative medicine, Baylor College of Medicine, Houston, Texas.

RNA isolation and RT-qPCR. RNA was isolated from snap-frozen liver tissue or cells by homogenization in TriZol reagent (Invitrogen) and precipitation with ethanol. cDNA was synthesized from 1 µg RNA using Qiagen's QuantiTect reverse transcription kit. Quantitative PCR was run on a Roche LightCycler 480 with Perfecta SYBR Green FastMix obtained from Quanta BioSciences (Gaithersburg, MD). Samples were run in duplicates and normalized to Tbp (mice), 36b4 (AML-12 cells) or Cyclophillin (C3HepG2 cells). Standard curves were ran for each primer set in each PCR run and relative fold changes were calculated with the ΔΔCt method. Primer sequences are available in Suppl. file 1.

Hydroxyproline assay. Referenced in (2). In brief, 200mg liver tissue were homogenized in 4ml of 6N HCL and boiled at 110°C for approximately 24h. After cooling down to ambient temperature the lysate was filtered and 50µl lysate were neutralized with 450µl of 2.2% citrate-acetate buffered NaOH. 500µl of buffered lysate were incubated with 250µl chloramine T solution (Sigma-Aldrich, St. Luis, MO) for 20 min, followed by incubation with 250µl perchloric acid for 10 min at room temperature. Finally, dimethylbenzaldehyde (Sigma-Aldrich, St. Luis, MO) solution was added for 20 min at 60°C. Samples and hydroxyproline (Sigma-Aldrich, St. Luis, MO) standard curve were measured at 565nm absorbance against blank solution.

Lipidomics. Liver tissues were homogenized in methanol and lipids extracted according to Folch et al. (3). Diheptadecanoyl-containing internal standards (PC 17:0/17:0 and PE 17:0/17:0) were added during the extraction and used for quantification. Phospholipids were

detected by multiple precursor ion scanning in negative mode using direct infusion on a QTRAP 5500 mass spectrometer (ABSciex, Concord, Canada,) equipped with a robotic nanoflow ion source TriVersa NanoMate (Advion Biosciences, Ithaca, NY, USA) according to previous work (4, 5).

Liquid Chromatography- Mass spectrometry. HPLC analysis was performed using an Agilent 1260 series HPLC system equipped with a degasser, binary pump, thermostatted autosampler and column oven (all from Agilent Technologies, Santa Clara, CA). The Mulitple Reaction Monitoring (MRM)-based measurement of levels of metabolites, that used a normal aqueous phase chromatographic separation, prior to mass spectrometry. For aqueous normal phase separation, a Diamond-Hydride column (100X2.1mm i.d.; 4.2µm particle size, Microsolve Technology Corporation, Eatontown, NJ) maintained at 37^{o}C, was used. The mobile phase used for this chromatographic separation contained acetonitrile (ACN, solvent A): water (solvent B), with both solvents modified by the addition of 0.2% Acetic acid and 0.1% formic acid, while the gradient conditions were 0-2 min-95%B; 3 min-90%B, 5 min-80%B, 6-7 min- 75%B, 8 min-55%B, 10 min-40%B, 12 min- 30%B, 14 min-20%B, followed by re-equilibriation to the initial starting condition. The flow rate was gradually increased during the separation from 0.5 mL/min (0-8 mins) to 0.7 mL/min (10-14 min) and finally set at 0.8 mL/min (15-17 min). The total run time was set to 20 min. The samples were kept at 4^{o}C and a constant volume of 5 µL was injected for analysis. The mass spectrometric analysis was performed on 6430 QQQ-LC/MS (Agilent Technologies, Santa Clara, CA). The mass spectrometer was operated in both electrospray positive ionization modes, with a capillary voltage of 3000 V, a collision gas flow rate of 10 L/min and a nebulizer gas flow rate of 35 L/min. The temperature of nebulizer gas was maintained at 350^{o}C. Nitrogen was used as the collision gas at a collision cell pressure of 2.39X10-^{5} Torr. For maximum sensitivity, the fragmentor voltage and collision energy for each metabolite were optimized separately using the optimizer® software (Agilent Technologies, Santa Clara, CA) and the optimized values were used for the Multiple Reaction Monitoring (MRM) assays. Sarcosine and alanine are isomeric compounds and have not been further separated by gas chromatography, therefore sarcosine represents both sarcosine and alanine isomeric compounds. Serum and hepatic amino acid levels were determined by mass-spectrometry-based methods in the Newgard lab (6).

Isolation and determination of hepatic triglycerides, cholesterol and non-esterified fatty acids. Lipid was extracted from mouse liver by homogenizing in 9 volumes PBS and was added to a chloroform:methanol (2:1) mixture. PBS was added and the samples were spun at 3000 rpm for 10 min at 4°C. The bottom layer was removed and solute evaporated overnight. Lipid was resuspended in 1% Triton-X in ethanol for 4 hr with rotation. This was then used to calculate liver triglycerides, cholesterol and non-esterified fatty acids using Thermo Scientific's (Waltham, MA) Infinity Triglyceride and Cholesterol kit and Wako's (Richmond, VA) NEFA kit, respectively.

H&E and Oil Red O staining. For H&E staining for conventional light microscopy, formalin-fixed livers were embedded in paraffin, and 4-mm–thick sections were stained with hematoxylin-eosin. For Oil Red O staining liver tissue was frozen in optimum cutting temperature compound (Sakura Finetek, Torrance, CA) on dry ice. Tissue was finely cut using a cryostat, fixed, and stained with Oil Red O solution.

Bile flow and biliary phospholipid / bile acid measurement. Bile flow and composition were determined in chow and MCD-fed WT and LRH-1$^{-/-}$ mice as previously described (7). Mice that were fasted overnight but had free access to water were anesthetized (10 mg of tribromoethanol intraperitoneally), and the gallbladder was cannulated after common bile duct ligation for collection of bile. After a 5-minute equilibration period, bile was collected in pre-weighed test tubes under mineral oil for 30 minutes, and bile flow was determined gravimetrically and normalized to liver weight as described previously. Biliary phospholipid concentration was determined using a commercially kit (Phospholipid C, Wako Chemicals, Richmond, VA). Biliary and serum bile acid concentration was determined by using a commercial kit (Total bile acid assay, Diazyme, Poway, CA).

Protein isolation and immunoblotting. Whole cell lysates were obtained from frozen liver tissue by mechanically disrupting tissue in RIPA buffer (150 mM sodium chloride, 1.0% Triton X-100, 0.5% sodium deoxycholate, 0.1% sodium dodecyl sulphate, 50 mM Tris, pH 8.0, 0.1mM EDTA) using a handheld homogenizer (Kinematica Polytron 1300D homogenizer, Fisher Scientific) followed by sonication for 30 seconds on ice. The resulting supernatant was collected and protein concentration was determined using the BCA protein assay kit (Pierce, Thermo Scientific, Rockford, IL). Samples were denaturated in sample buffer (NuPage LDS sample buffer, Invitrogen, Carlsbad, CA), boiled for 10 minutes and separated on 4–12% Bis-Tris gels (Invitrogen, Carlsbad, CA). 50 µg of total protein was loaded. The following antibodies and conditions were used: Gnmt (AP1076b; 1:500; Abgent, San Diego, CA), b-Actin (sc-1616 HRP; 1:3000; Santa Cruz Biotechnology, Dallas, TX). Immobilon Western substrate (Millipore, Billerica, MA) was used for detection.

Microarray analysis. Microarray analysis was performed as described previously (8). In brief, pooled total RNA from liver tissue of chow and MCD-fed WT and LRH-1$^{-/-}$ mice (n=3 per group) was reverse transcribed using the Illumina TotalPrep RNA Amplification Kit (Ambion, Austin, TX) and hybridized to the Illumina mouseRefseq-8v2 Expression BeadChip using standard protocols (Illumina, San Diego, CA). Chips were run in dublicates. Arrays were normalized with Chipster software (9) using default settings for Illumina arrays. Genes upregulated >0.80log2 (>1.74-fold) and downregulated >log2-0.80 (<0.57-fold) were regarded as significant and further analyzed.

Determination of LRH-1 binding sites. For genome-wide binding of LRH-1, we obtained a BED file from the lab of Tim Osborne (10) and annotated distance to TSS using Galaxy / Cistrome (www.cistrome.org) (11).

siRNA knockdown of LRH-1 and DLPC treatment. Experiments were performed in AML-12 cells at 70-80% confluency in 24-well plates. 3 different LRH-1 or scrambled siRNAs were purchased from Invitrogen (Stealth siRNA). 50 pmol of pooled siRNA was transfected into each well using Lipofectamine RNAiMAX transfection reagent (Invitrogen). Cells were harvested 48h after transfection to isolate total RNA. For experiments using dilauroyl-sn-glycero-3-phosphocholine (DLPC) treatment, cells were treated with 100mmol DLPC (Avanti Polar Lipids, Alabasta, Alabama) for 24h.

Gnmt promotor luciferase assay and site directed mutagenesis. GNMT promoter cloning included the sequence from nucleotides -26 to -658 upstream of the GNMT transcription start site and was cloned into Promega's pGL4.21 [*luc2P*/Puro] vector (cat# E676A). A single canonical LRH-1 binding site was located at -143 from TSS and a non-canonical binding site

at -68 from TSS. For site directed mutagenesis a deletion of 17 bp completely deleting the canonical LRH-1 binding site and a 2bp deletion in the center of the non-canonical binding site was generated using the Kapa Hifi site-directed mutagesis protocol (http://www.kapabiosystems.com/assets/KAPA_HiFi_Site_Directed_Mutagenesis_Note.pdf) with the modification of 20 cycles of mutagenesis PCR. Positive colonies were minipreped, PCRed and the resulting PCR control digested with Sml I which cuts within the LRH-1 site. Restriction digest negative clones were sequenced and deletion verified. Gnmt promotor primer with NheI cut site fw: 5' ATGA[GCTAGC]ATGGAAAGCAGATGGAAGG 3' and Gnmt promotor primer with HindIII cut site rev: 5' AGTC[AAGCTT]ACGCGATCCGCACTTA 3'; GNMT mut-143 fw: 5'AGAGGCAGCAAGCCTGGC3' and GNMT mut-143 rev: 5'AGGATGGCTCAGCACAGCAATC3'. Luciferase assay was performed following the Promega Luciferase assay protocol (cat# E4030) using reporter lysis buffer (RLB). Briefly, cells were seeded in 12-well plates, the next day triple transfected with the GNMT promoter construct with or without deletion, a beta-Gal plasmid and increasing concentrations (0-600ng) of LRH-1 plasmid. Triplicate wells were transfected for each LRH-1 concentrations. After 24h cells were harvested in 200ul RLB and a single freeze-thaw cycle. Cells were scraped off, centrifuged and 20ul lysate was used for luciferase assay. The assay was performed in a plate reading luminometer with injector in duplicates and 100ul luciferase reagent was injected with measurments taken every second for 10 seconds. B-Gal assay was performed following the Promega protocol (cat# E2000). A standard curve was prepared as indicated in the manual. 30ul lysate from the above mentioned samples was mixed with 20ul RLB and after the addition of 50ul assay buffer (2x) incubated for 30min at 37C. Duplicate well measurements were performed. Then the reaction was stopped with 150ul 1M sodium carbonate. Absorbance was read immediately at 420nm.

LRH-1 reporter luciferase assay. Luciferase assays were performed with extracts of C3HepG2 cells plated in 24-well plates and transfected with 200ng expression plasmids for human LRH-1 or CAR, 200ng LRH-1/SF-1 Luc reporter plasmid or LXR/DR4 CAR reporter plasmids (12), respectively and 150ng b-galactosidase. 24h later cells were incubated with regular DMEM/F-12 media or custom made MCD media (see above) for different time points and concentrations. After 12h or at given timepoints (timecourse experiments) cells were lysed and luciferase and β-galactosidase activity measured (8). Luciferase expression was normalized by β-galactosidase expression.

Chromatin immunoprecipitation (ChIP) for mouse and human LRH-1 binding sites. Livers of WT and LRH-1$^{-/-}$ mice fed with either chow or 2 weeks of MCD diet (3 per group) and pooled tissue from human liver wedge biopsies, which served as normal control samples in a previous study (13) were processed for ChIP experiments. The commercially available kit ChIP-IT® High Sensitivity (Active Motif, Inc., Carlsbad, CA) was used. The protocol followed the instructions provided by the kit with minor modifications. Shearing efficiency was tested on 2% agarose gel with 750ng DNA per well. The mean smear appeared between 200bp – 800bp suggesting efficient shearing. For immunoprecipitation 5µg of anti-LRH-1 antibody (R&D Systems, Abingdon, UK, #PP-H2325-00) and 2-3mg sheared chromatin were used. Human DNA was eluted in 36µl DNA Purification Elution Buffer and murine DNA in 60µl. Subsequent quantitative PCR was performed using the ChIP-IT® qPCR Analysis Kit (Active Motif, Inc., Carlsbad, CA) on a Light Cycler 480 (Roche Diagnostic, Rotkreuz, Switzerland). The protocol followed the instructions provided by the kit. Amplification

conditions were optimized and are as follows: 45 cycles [95°C (10 seconds), 56°C/58°C (20 seconds), 72°C (1 second)] with KAPA SYBR® FAST qPCR Master Mix (Kapa Biosystems, Wilmington, MA) for primers with an optimal annealing temperature of 56°C or 58°C. 45 cycles [95°C (15 seconds), 60°C (1 minute)] with SYBR® Green PCR Master Mix (Applied Biosystems, Waltham, MA) for primers with an optimal annealing temperature of 60°C. All samples were run in triplicates. Primer pairs spanning established LRH-1 binding sites (Cyp7a1, Cyp8b1, CYP7A1, CYP8B1, ABCG5/8, CETP) served as positive controls. All values were normalized to the mean of the negative control. Primers for ChIP PCR are provides in suppl. table 2.

Statistical analysis. Numbers of mice or replicates for each group used in experiments are indicated in the figure legends. For statistical analysis, analysis of variance with Bonferroni posttesting (experiments with animals and primary hepatocytes) and Student *t* test (cell line experiments) was used (Sigmastat statistic program; Jandel Scientific, San Rafael, CA). A *p* value of less than .05 was considered significant. For statistical analysis of microarray experiments hypergeometric testing relative to the total numbers of transcripts and genes on the Illumina mouseRefseq-8v2 Expression BeadChip (see above) was performed using R software. Error bars represent means ± standard deviation.

Supplementary figure legends.

Suppl. figure 1. Wildtype (WT) and liver specific LRH-1 knockout (LRH-1$^{-/-}$) mice were fed MCD diet for 2 weeks. **A.** Imaging: H&E staining (upper panel) and Oil-red O staining (lower panel) of MCD-fed WT and MCD-fed LRH-1$^{-/-}$ mice showing comparable amounts of macrovesicular steatosis. Quantification of hepatic triglycerides (left graph), hepatic cholesterol (middle graph) and hepatic free fatty acids (right graph) does not show differences in hepatic lipid content between WT and LRH-1$^{-/-}$ mice. n=6-8 mice per group. **B.** Loss of body weight per 100g mouse (left graph). Both, WT and LRH-1$^{-/-}$ mice significantly lose weight after MCD feeding, with a trend for more weight loss in MCD-fed WT mice. There is no difference in liver to body-weight ratio. n=6-8 mice per group. * $p<0.05$, chow vs. MCD. Error bars represent means ± standard deviation. **C.** Serum levels of hepatic injury markers ALT and LDH (n=5 mice per group serum levels).

Suppl. figure 2. Wildtype (WT) and liver specific LRH-1 knockout (LRH-1$^{-/-}$) mice were fed MCD diet for 2 weeks. Comprehensive mass-spectrometry based lipidomics analysis of PC classes **(A)** and Lyso-phosphatidylcholines (Lyso-PCs) **(B)**. Lyso-PCs are only significantly increased in MCD-fed WT mice and remain at normal levels in MCD-fed LRH-1$^{-/-}$ mice. n=5-6 mice per group. Error bars represent means ± standard deviation.

Suppl. figure 3. Wildtype (WT) and liver specific LRH-1 knockout (LRH-1$^{-/-}$) mice were fed MCD diet for 2 weeks. **A.** Mass-spectrometry based analysis of serum and hepatic levels of methionine, glycine, serine and hepatic methyltetrahydrofolate shows reduction of methionine levels in MCD-fed LRH-1$^{-/-}$ mice and induction of glycine and serine levels (hepatic glycine levels are a repeated measurement of hepatic glycine levels of Figure 3c of the main text and therefore slightly differ). Heptatic methyltetrahydrofolate levels remain unchanged. **B.** Mass-spectrometry based analysis shows significantly reduced levels of betaine as direct breakdown product of choline after feeding MCD diet in WT and LRH-1$^{-/-}$ mice. n=3-4 mice per group.

Suppl. Figure 4. mRNA levels of the main enzymes involved in methyl-pool metabolism as referenced in (14). n=7-9 mice per group.* $p<0.05$, chow vs. MCD; $^{\#}$ $p<0.05$, WT vs. LRH-1$^{-/-}$. Error bars represent means ± standard deviation.

Suppl. figure 5. A. C3HepG2 cells were transfected with a LXR/DR4 CAR luciferase reporter, b-galactosidase and either hCAR or a corresponding empty vector (ev) and incubated for 12h with regular DMEM/F-12 media or custom-made identical media depleted of methionine and choline (MCD media). n=triplicates. **B.** C3HepG2 cells were incubated with control or MCD media for the indicated time points and viability was measured using a MTT assay. n=sextuplicates. * $p<0.05$, control media vs MCD media. Error bars represent means ± standard deviation.

Suppl. figure 6. A. Serum and biliary bile acid levels were determined in WT and LRH-1$^{-/-}$ mice on chow and MCD-diet. MCD diet induces a modest significant induction of serum biled levels only in WT-MCD fed mice. Biliary bile acid output is significantly induced in both genotypes upon MCD-feeding. **B.** mRNA levels of canalicular (Mrp2 and Bsep) and basolateral (Mrp3, Mrp4 and Ostb) as well as of bile acid metabolizing enzymes (Cyp8b1 and Cyp7a1) have been determined by RT-PCR. n=5 mice per group.* $p<0.05$, chow vs. MCD; $^{\#}$ $p<0.05$, WT vs. LRH-1$^{-/-}$. Error bars represent means ± standard deviation.

Suppl. figure 7. Schematic on the proposed effects of MCD diet in WT and LRH-1$^{-/-}$ mice. MCD diet results in significant decrease of the PC/PE ratio and SAM pools in WT mice resulting in liver injury resembling non-alcoholic steatohepatitis. LRH-1$^{-/-}$ mice display reduced expression of the biliary phospholipid floppase Mdr2, thereby limiting biliary PC loss, and reduced expression of the main methyltransferase Gnmt, thereby limiting SAM breakdown. These effects result in maintenance of a critical PC/PE ratio and SAM pool and lead to reduced liver injury in MCD-fed LRH-1$^{-/-}$ mice.

References

1. Lee YK, Schmidt DR, Cummins CL, Choi M, Peng L, Zhang Y, et al. Liver receptor homolog-1 regulates bile acid homeostasis but is not essential for feedback regulation of bile acid synthesis. Mol Endocrinol 2008;22:1345-1356.
2. Jamall IS, Finelli VN, Que Hee SS. A simple method to determine nanogram levels of 4-hydroxyproline in biological tissues. Anal Biochem 1981;112:70-75.
3. Folch J, Lees M, Sloane Stanley GH. A simple method for the isolation and purification of total lipides from animal tissues. J Biol Chem 1957;226:497-509.
4. Ejsing CS, Duchoslav E, Sampaio J, Simons K, Bonner R, Thiele C, et al. Automated identification and quantification of glycerophospholipid molecular species by multiple precursor ion scanning. Anal Chem 2006;78:6202-6214.
5. Jung HR, Sylvanne T, Koistinen KM, Tarasov K, Kauhanen D, Ekroos K. High throughput quantitative molecular lipidomics. Biochim Biophys Acta 2011;1811:925-934.
6. Batch BC, Shah SH, Newgard CB, Turer CB, Haynes C, Bain JR, et al. Branched chain amino acids are novel biomarkers for discrimination of metabolic wellness. Metabolism 2013;62:961-969.
7. Fickert P, Wagner M, Marschall HU, Fuchsbichler A, Zollner G, Tsybrovskyy O, et al. 24-norUrsodeoxycholic acid is superior to ursodeoxycholic acid in the treatment of sclerosing cholangitis in Mdr2 (Abcb4) knockout mice. Gastroenterology 2006;130:465-481.
8. Mamrosh JL, Lee JM, Wagner M, Stambrook PJ, Whitby RJ, Sifers RN, et al. Nuclear receptor LRH-1/NR5A2 is required and targetable for liver endoplasmic reticulum stress resolution. Elife 2014;3:e01694.
9. Kallio MA, Tuimala JT, Hupponen T, Klemela P, Gentile M, Scheinin I, et al. Chipster: user-friendly analysis software for microarray and other high-throughput data. BMC Genomics 2011;12:507.
10. Chong HK, Biesinger J, Seo YK, Xie X, Osborne TF. Genome-wide analysis of hepatic LRH-1 reveals a promoter binding preference and suggests a role in regulating genes of lipid metabolism in concert with FXR. BMC Genomics 2012;13:51.
11. Liu T, Ortiz JA, Taing L, Meyer CA, Lee B, Zhang Y, et al. Cistrome: an integrative platform for transcriptional regulation studies. Genome Biol 2011;12:R83.
12. Tzameli I, Pissios P, Schuetz EG, Moore DD. The xenobiotic compound 1,4-bis[2-(3,5-dichloropyridyloxy)]benzene is an agonist ligand for the nuclear receptor CAR. Mol Cell Biol 2000;20:2951-2958.
13. Marschall HU, Wagner M, Zollner G, Fickert P, Diczfalusy U, Gumhold J, et al. Complementary stimulation of hepatobiliary transport and detoxification systems by rifampicin and ursodeoxycholic acid in humans. Gastroenterology 2005;129:476-485.
14. Lu SC, Mato JM. S-adenosylmethionine in liver health, injury, and cancer. Physiol Rev 2012;92:1515-1542.

15. Wagner M, Halilbasic E, Marschall HU, Zollner G, Fickert P, Langner C, Zatloukal K, Denk H, Trauner M. CAR and PXR agonists stimulate hepatic bile acid and bilirubin detoxification and elimination pathways in mice. Hepatology. 2005 Aug;42(2):420-30.

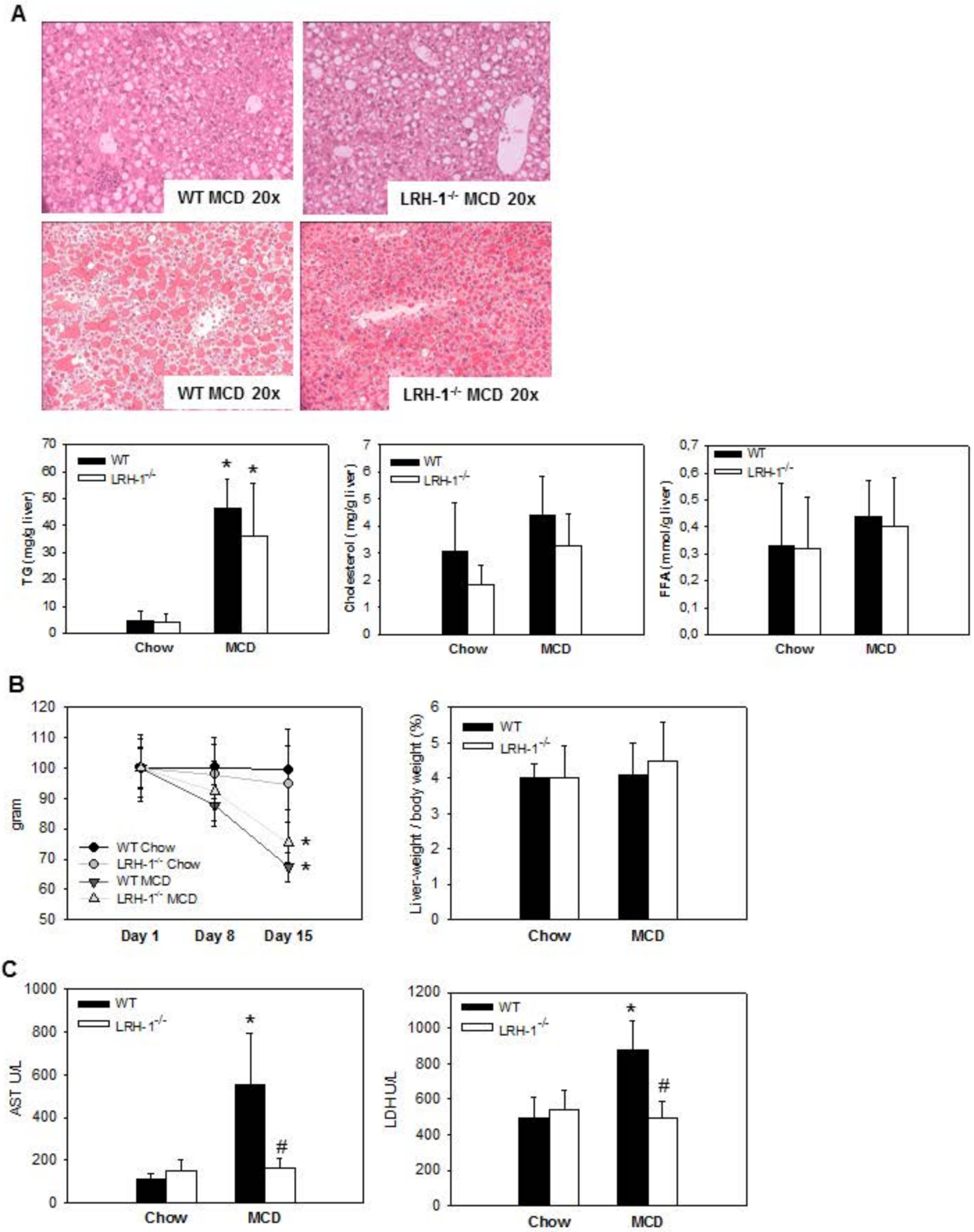

Suppl. figure 1

A

	Ctrl Chow	LKO Chow	Ctrl MCD	LKO MCD
PC 16:0/18:2	4.57	4.14	2.24	2.54
PC 16:0/20:4	2.14	1.86	1.45	1.48
PC 18:0/18:2	2.00	2.02	1.43	2.03
PC 18:0/20:4	1.81	1.46	1.74	1.59
PC 16:0/18:1	1.03	1.25	0.58	0.62
PC 16:0/22:6	0.57	0.48	0.49	0.47
PC 18:1/18:2	0.40	0.54	0.39	0.39
PC 18:1/20:4	0.35	0.34	0.23	0.20
PC 16:0/16:0	0.27	0.32	0.30	0.31
PC 18:0/22:6	0.26	0.21	0.33	0.28
PC 16:0/20:3	0.25	0.23	0.14	0.17
PC 18:2/18:2	0.24	0.32	0.22	0.28
PC 18:2/20:4	0.24	0.28	0.14	0.19
PC 18:0/18:0	0.22	0.16	0.11	0.12
PC 18:0/18:1	0.22	0.26	0.15	0.19
PC 18:0/20:3	0.20	0.17	0.17	0.18
PC 16:1/18:2	0.16	0.19	0.12	0.14
PC 16:0/18:0	0.13	0.13	0.11	0.12
PC 16:0/18:3	0.12	0.09	0.10	0.06
PC 16:0/20:2	0.12	0.11	0.15	0.16
PC 16:0/22:5	0.12	0.21	0.08	0.10
PC 16:0/16:1	0.09	0.11	0.08	0.09
PC 14:0/16:0	0.06	0.14	0.08	0.12
PC 18:0/22:5	0.06	0.10	0.06	0.06
PC 18:0/20:2	0.06	0.06	0.13	0.13
PC 18:1/18:1	0.05	0.09	0.06	0.06
PC 18:2/20:0	0.05	0.03	0.01	0.02
PC 16:1/20:4	0.05	0.06	0.04	0.04
PC 16:1/18:1	0.05	0.06	0.04	0.04
PC 18:1/20:3	0.03	0.04	0.02	0.02
PC 18:2/20:3	0.03	0.04	0.02	0.02
PC 20:0/20:4	0.03	0.02	0.01	0.01
PC 18:2/20:1	0.03	0.03	0.02	0.02
PC 18:2/18:3	0.03	0.03	0.03	0.03
PC 16:0/20:1	0.03	0.04	0.03	0.03
PC 14:0/18:2	0.03	0.03	0.03	0.04
PC 16:1/18:0	0.03	0.03	0.03	0.03
PC 18:2/20:2	0.03	0.03	0.02	0.02
PC 18:1/20:2	0.02	0.03	0.04	0.05
PC 20:1/20:4	0.02	0.02	0.01	0.01
PC 20:2/20:4	0.02	0.02	0.01	0.01
PC 18:0/18:3	0.02	0.02	0.03	0.02
PC 14:0/20:4	0.02	0.02	0.01	0.01

B

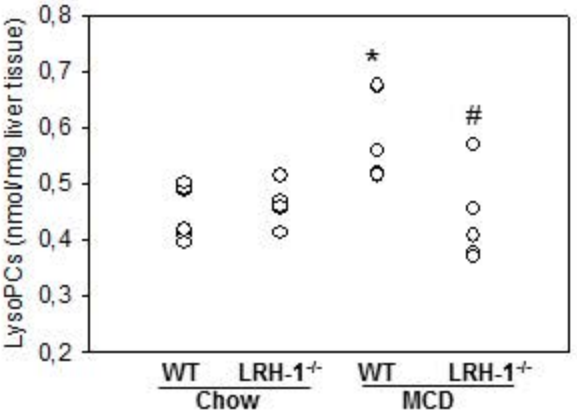

Suppl. figure 2

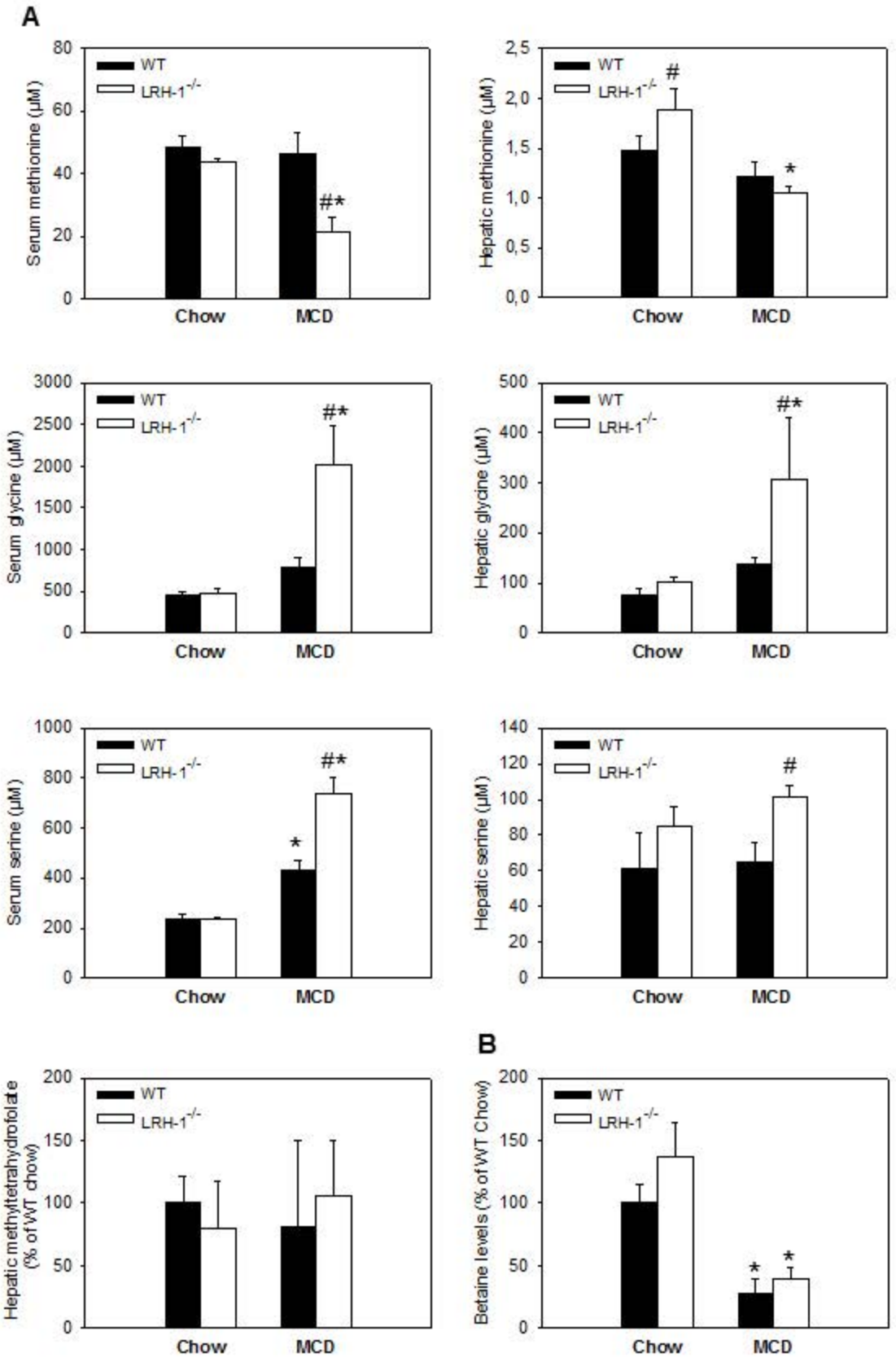

Suppl. figure 3

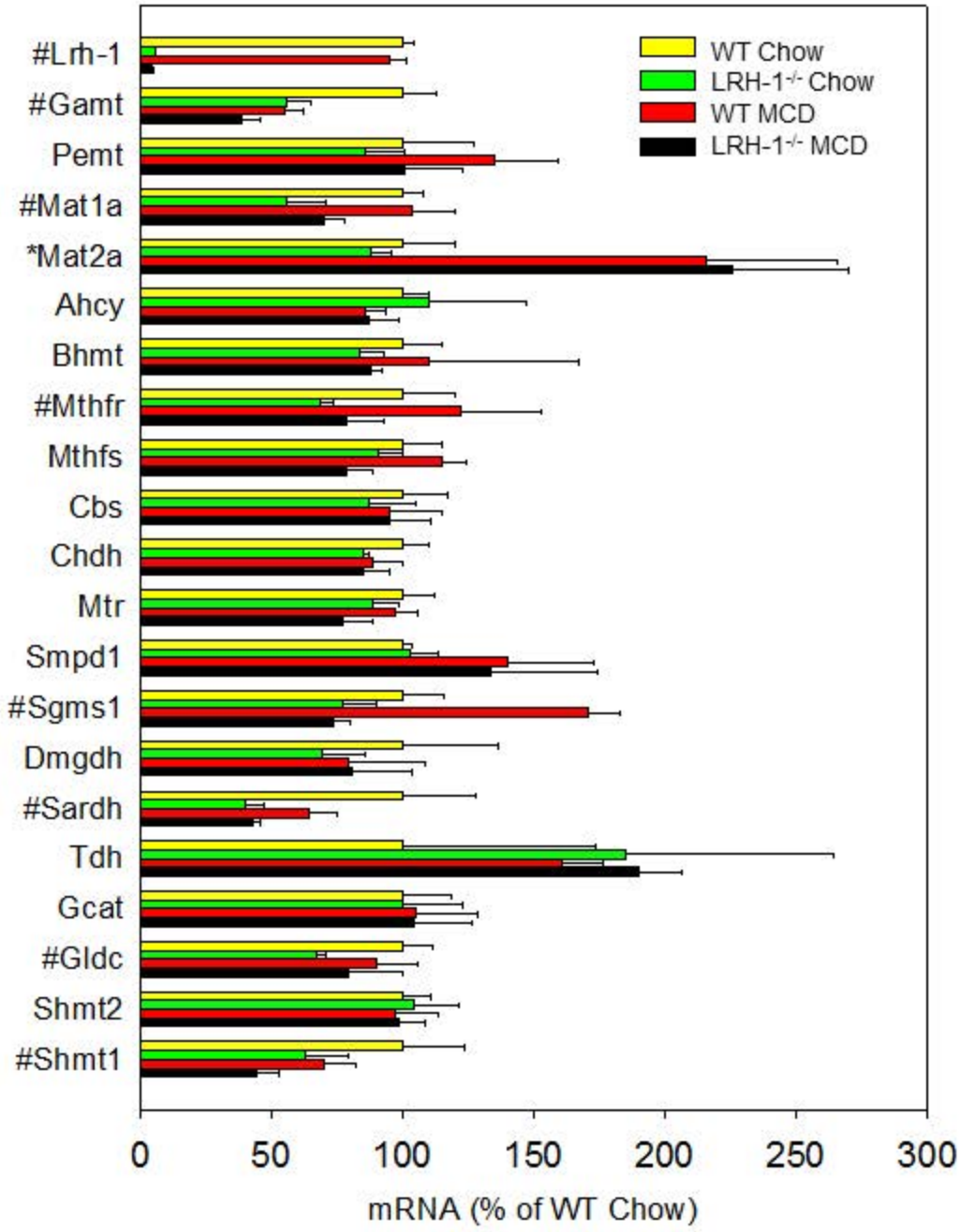

Suppl. figure 4

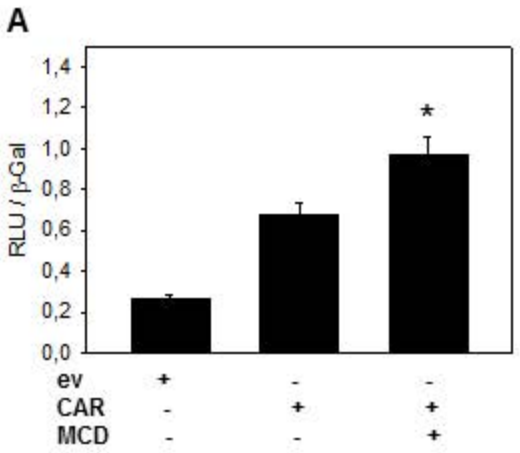

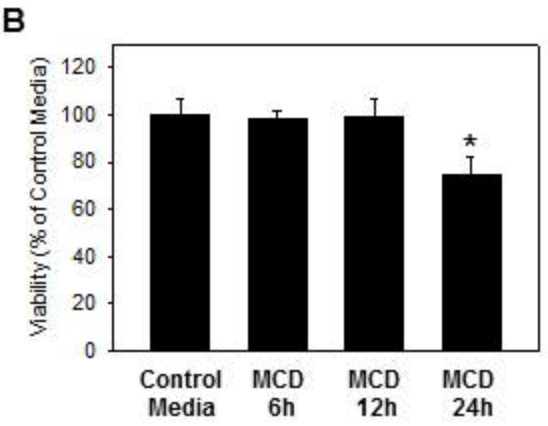

Suppl. figure 5

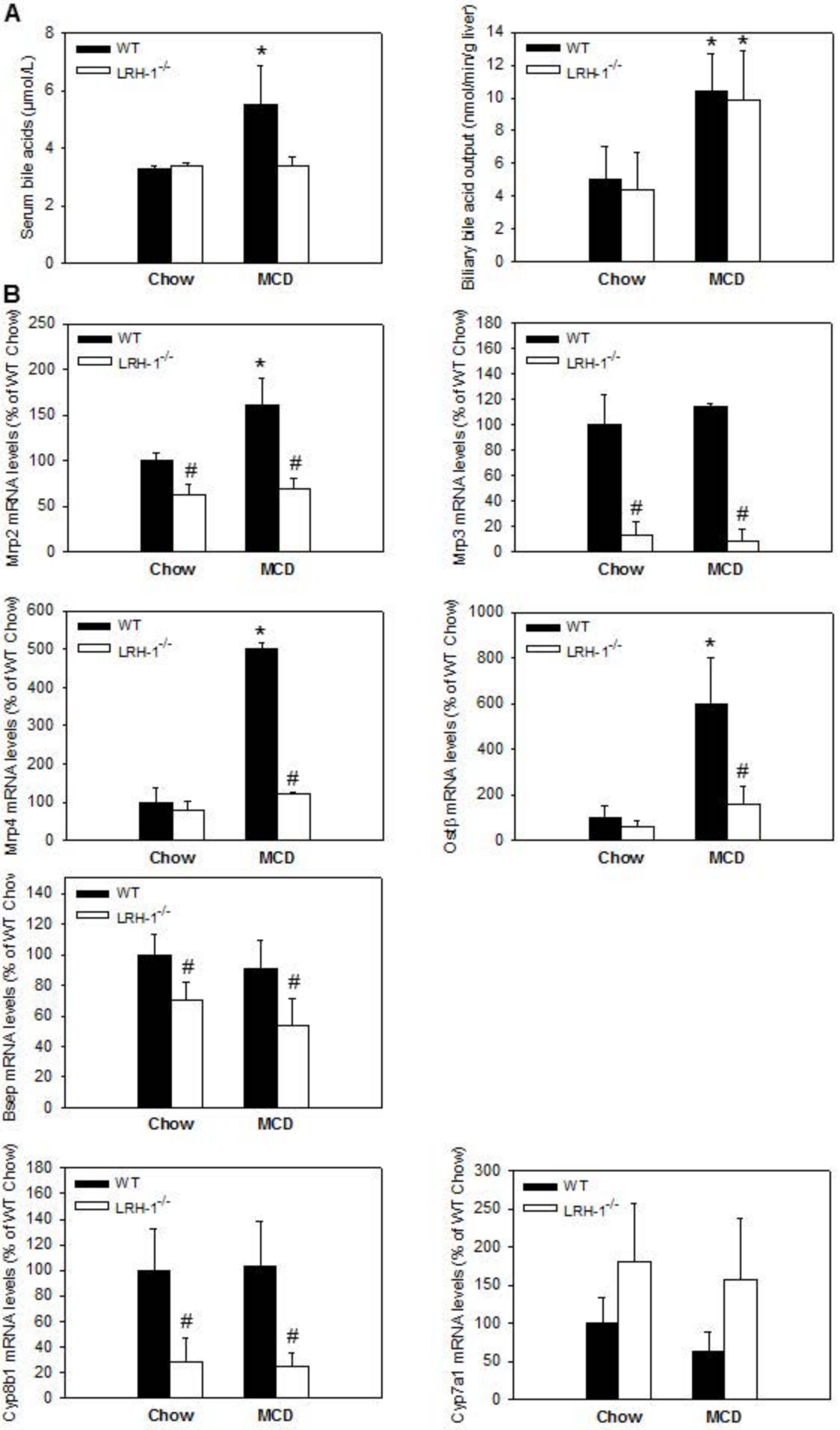
A
Serum bile acids (μmol/L)
WT
LRH-1-/-
Chow
MCD
Biliary bile acid output (nmol/min/g liver)
B
Mrp2 mRNA levels (% of WT Chow)
Mrp3 mRNA levels (% of WT Chow)
Mrp4 mRNA levels (% of WT Chow)
Ostβ mRNA levels (% of WT Chow)
Bsep mRNA levels (% of WT Chow)
Cyp8b1 mRNA levels (% of WT Chow)
Cyp7a1 mRNA levels (% of WT Chow)

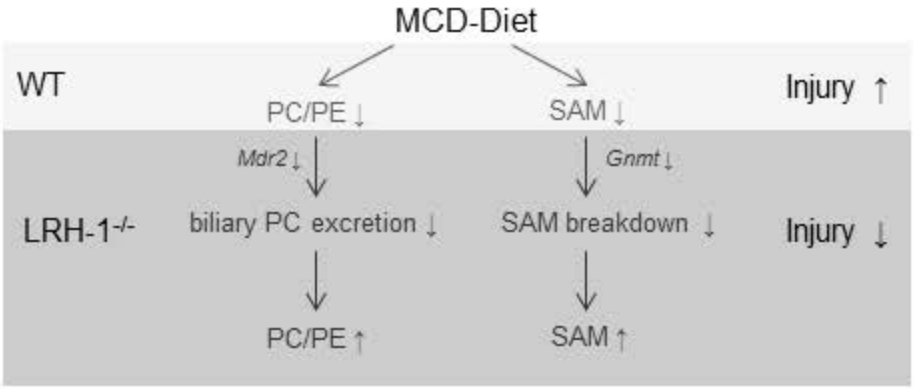

Suppl. figure 7

Suppl. Table 1. Forward and reverse primer sequences for RT-qPCR. Human Genes are capitalized. Primers for bile acid transporters and bile acid enzymes are referenced in Suppl. 15.

Gene	forward primer	reverse primer
36b4	ataaccctgaagtgctcgacat	gggaaggtgtactcagtctcca
Ahcy	aacctcatccacaccaaatacc	acagaatcgttgacattgatgg
Bhmt	cactcactacaccggaaagatg	aagacaaatcctccatctccaa
Cbs	tctgcaaagtcctctacaagca	ctccaggatgtgagagagtgtg
Chdh	cagtaggtgtggagtacatcaagg	agtttcctgaggtcatctgcat
Col1a1	cctcagggtattgctggacaac	accacttgatccagaaggacctt
CYCLOPHILIN	ggagatggcacaggaggaa	gcccgtagtgcttcagttt
CYP7A1	gcgactttctggagtttatttca	tttcattgcttctgggttcc
Cyp8b1	gccttcaagtatgatcggttcct	gatcttcttgcccgacttgtaga
CYP8B1	tggtgctgaaggtatttgga	tggtgctggctgagtgtatc
Dmgdh	agaggtcgggtgtatgctga	aaggctgcttcttcaatcca
Gamt	tccaaatacacagacatcacca	gatcatctgagggaaggcatag
GAMT	cacggcagacacacaaggt	tccgagagtgggtacgtgt
Gcat	acctggaagagtgagcgtgt	ttggcacagaagttgaggatt
Gldc	atcctcgttgtcacccaca	cgtctttgccactgaaatcc
Gnmt	gtgctggacgtagcctgtg	atcacgctgaagccctctt
GNMT	gccagtgacaagatgctgaa	atcaaagccaccctctgct
Icam	agggctggcattgttctcta	cttcagaggcaggaaacagg
Lrh-1	gtgtggcgataaagtgtctg	ttggcaattctggttctctatg
Mat1a	gacaccatcaagcacattgg	ctgcaccaacatcctcttca
Mat2a	ccttggttacgcccagatt	ccttcagagcatccctcatc
Mdr2	gtgaagagtggacagacagtgg	gatttcccttagacacctgacg
MDR3	ccctactttgtcgtgggaac	cacttctgctgcttcactgc
Mthfr	ggaccgagtttgctgactattt	ttctccttcaaatgcttcaggt
Mthfs	tctctcctcctcacgcagaa	tccgtctcaacttcatcttgc
Mtr	ttggaaaatgtacaacagcctatgtc	tttcatcatagtcgccaaaagtgt
Pemt	tccttctggttctggctgat	agttctctgctcccatctcg
Sardh	actcggttgtcttcccacac	atccctgtcgctcttgaaac
Sgms1	catgctaacgctcacctaccta	tagtggtcatgcgctaagagaa
Shmt1	gaatgccagcctcttccac	ccgtgcgtagtccaggtt
Shmt2	acattggcttggaggtgaag	ctgggtctttgagcaggaag
Smpd1	gcccagtgctacaacctttatc	agatgtaggtctcgtggtccag
Tbp	gaagctgcggtacaattccag	ccccttgtaccttcaccaat
Tdh	gatgccaacttccactccac	cattgtccttcccaaatcgt
Tnfa	catcttctcaaaattcgagtgacaa	tgggagtagacaaggtacaaccc

Suppl. Table 2. Forward and reverse primer for LRH-1 ChIP PCR.

	forward primer	**reverse primer**
human		
hABCG5/8	**CCAGCGCGTCCTTATCTTGA**	**GCTCTCTTAGACCCAGCTGC**
hCETP	**TGGTGGAGGGGAGACAAGTA**	**CCCGTATATGTATGTCCGCCC**
hCYP7A1	TTAGCTGTTGTCCCCAGGTC	TCCATTAACTTGAGCTTGGTG
hCYP8B1	TTACCTCCTCCTCCCCTACG	GCGGATTAAGCTCTCGACAC
hGNMT -705	GGCCAACACGCGCGT	GATTAGCTGGGACATGGTGACAC
hGNMT -1290	**CAGTTGCTTCCATGTTTAGGC**	**CCTTCCTTTCCAACTTGGG**
hGNMT -1700	**AAAGGCTAAACCTCCCCAG**	**CCTTTGGTACTGTTTGGCC**
hGNMT -1950	**CTCACTGCAACCTCTGCCA**	**CGTGCCTGTAATCCCAGCTAC**
hMDR3 -1450	**GCACCTGCTATGTCCTGTTAACAC**	**ATGCTCTGCTTTAAGGTTCTCTGAG**
mouse		
mCyp7a1	**ATAGCATTATCTGGCCTTGAACTAAG**	**GTAGGTGAGCTCTTCTGTAGTGTGTTTAC**
mCyp8b1	**AGGTTGTGTGCCAGCTGTGC**	**TAGCCAATGAACTGAGGTGTGAATG**
mGnmt -143	CTGGCGAGTCCTATCTGACC	TAATCCTCTGGCAAGGCAGT

LRH-1-/- chow vs WT chow			
gene name	fold up	gene name	Fold down
CYP4A12A	39,43	APON	0,09
TFF3	37,09	A1BG	0,09
CYP2D12	29,90	HAMP2	0,12
CYP4A12B	12,83	MRAP	0,16
EIF2S3Y	11,48	ALDH1B1	0,18
OLIG1	11,03	ANG	0,21
Mup21	10,84	MMD2	0,23
Gm4956	10,41	SERPINC1	0,25
Serpina4-Ps1	6,92	SULT3A1	0,26
Nat8	5,96	OAT	0,26
AKR1C19	5,87	ABCC3	0,27
ESPN	5,64	PAQR9	0,29
CYP2D9	5,55	ST3GAL6	0,29
CYP2C55	5,46	ACOT1	0,30
CHRNA4	4,61	ARHGEF19	0,31
TINAG	4,36	CYP2C39	0,31
SPP1	4,15	VLDLR	0,31
HSD3B5	4,15	ORM2	0,32
CFD	4,09	AGPAT2	0,32
NTRK2	4,04	D14ERTD449E	0,33
CORIN	4,02	SULT5A1	0,33
SPINK3	4,02	DCT	0,33
NOX4	3,97	RCAN2	0,33
SFTPD	3,84	ORM1	0,34
ALAS2	3,80	CYP8B1	0,34
SLPI	3,70	CYP4A31	0,34
GPC1	3,65	RHBG	0,34
C6	3,49	Gm4952	0,36
ABCB1B	3,43	GDF15	0,37
PDE6C	3,39	CCBL2	0,37
GAL3ST1	3,03	HGFAC	0,38
AACS	3,01	NT5E	0,38
Ifi27l2b	2,99	SLC25A25	0,38
BDH2	2,98	LOC100047200	0,38
BEX4	2,95	TDO2	0,38
DDX3Y	2,91	CAR3	0,38
RBP1	2,89	TBX3	0,39
CYP2B10	2,89	INSIG2	0,39
IGFBP5	2,87	SERPINA6	0,41
EPDR1	2,86	CTSC	0,41
TSPAN8	2,86	LOC100047173	0,41
AGXT2L1	2,85	RNASE4	0,42
GSTA2	2,83	HACL1	0,42
TMC5	2,78	ABCG5	0,42
C9	2,75	MT2	0,43
OMD	2,74	LOC100047762	0,43
AKR1B10	2,67	PLK3	0,43
MFGE8	2,61	NTN2L	0,43
Mup20	2,60	RFX4	0,43
GSTP1	2,58	AI132487	0,43
LOC626152	2,55	ABCG8	0,44
SUCNR1	2,55	TMPRSS2	0,44
CTSA	2,52	CSAD	0,44
PDZK1IP1	2,51	SLC13A2	0,44
SMPD3	2,47	SLC15A2	0,45
CXCL14	2,46	CYP2C37	0,45
AQP4	2,45	ACPP	0,46

LOXL1	2,45	IGFBP1	0,46
DPT	2,43	OAF	0,46
AQP8	2,43	GJB2	0,46
CYP7B1	2,43	ANG2	0,46
S3-12	2,40	ITIH3	0,47
EVC	2,38	SPHK2	0,47
S100A11	2,35	KRT75	0,47
MYL1	2,35	ACSL1	0,47
OLFM3	2,33	SLC16A10	0,47
BICC1	2,33	LBP	0,48
EFHA1	2,33	FCER1G	0,48
SCARA3	2,27	PLG	0,48
ANK3	2,26	CRIP2	0,48
KLK1B4	2,25	FGL1	0,48
SERPINE2	2,24	GCK	0,48
CDH1	2,23	SLC22A1	0,48
CCDC120	2,23	INHBE	0,48
FMN2	2,22	PNPO	0,48
USP2	2,21	UCK1	0,48
ACPL2	2,20	CRYBB3	0,49
SCAMP5	2,19	TSPAN31	0,49
CRYL1	2,18	ACOT3	0,49
ID1	2,17	MREG	0,49
ALDOC	2,17	ATF5	0,49
STEAP2	2,17	NAGS	0,50
UPP1	2,17	CIB2	0,50
CIDEC	2,16	AGT	0,50
COL1A1	2,13	SAS	0,50
TREH	2,13	VSIG4	0,50
CCDC3	2,13	HSPA8	0,50
RND2	2,12	ST6GAL1	0,50
LOC641240	2,12	H19	0,50
ALDH1A7	2,11	CD1D1	0,50
ACLY	2,11	GNPDA1	0,50
CRYM	2,09	PLA1A	0,50
MMP15	2,08	DUSP6	0,50
SERPINA11	2,08	DHRS7	0,51
CCL21A	2,08	ABHD2	0,51
LY6E	2,07	GULO	0,51
UAP1L1	2,05	UBE2U	0,51
AI428936	2,04	QPCT	0,51
SCARA5	2,04	HSD3B7	0,52
PPP1R14A	2,03	CLPX	0,52
RANBP3L	2,02	CSRP3	0,52
USP20	2,02	IL1RN	0,52
GAS6	2,02	EHHADH	0,52
NUDT7	2,02	ACAT1	0,52
RDHE2	2,01	RETSAT	0,52
HIST1H1C	2,01	NELF	0,52
MVP	2,01	HSPA5	0,52
SRD5A1	2,00	PAOX	0,53
KRT8	1,99	HSPB8	0,53
CYB561	1,99	GLUL	0,53
TCEAL5	1,99	FGF1	0,53
MTMR11	1,98	NDRG2	0,53
SLCO2A1	1,98	SCARB1	0,53
SPATA24	1,98	MUG2	0,54
ARSA	1,98	ABHD1	0,54
HBB-B2	1,98	SLC1A2	0,54

FOXQ1	1,97	MRPL15	0,54
9130409I23RIK	1,97	SYBU	0,54
BOK	1,96	ACOT4	0,54
SORT1	1,96	LOC100047579	0,54
AOX3	1,95	CTH	0,54
SNX15	1,95	PAPSS2	0,54
AU040829	1,95	PSEN2	0,54
HSPA2	1,95	TGOLN1	0,55
F2R	1,95	EPAS1	0,55
EVC2	1,95	SLC2A2	0,55
H2-AB1	1,95	MIF4GD	0,55
FMR1NB	1,94	MCFD2	0,55
MTNR1A	1,94	PCK1	0,55
H2-M2	1,94	ARNTL	0,55
RAB34	1,94	CLDN2	0,55
JARID1D	1,93	CRAT	0,55
LOC100043671	1,93	SLC23A2	0,55
GSTA1	1,93	CYP17A1	0,55
HSPBAP1	1,93	RGS12	0,55
ARSG	1,92	CYP3A25	0,56
MMP2	1,92	SLCO1B2	0,56
MUP5	1,91	ECI3	0,56
OLFML1	1,91	SLC25A20	0,56
WNT5B	1,90	ABHD3	0,56
SFXN1	1,90	HP	0,56
GM129	1,90	TSSC1	0,56
NENF	1,89	CAMK1D	0,56
TMEM51	1,89	CYP4A14	0,56
MYH10	1,89	CYP2C38	0,56
A230050P20RIK	1,88	LMNA	0,56
PTPRE	1,88	GBP3	0,56
SELENBP2	1,88	CYP3A11	0,56
ENTPD2	1,88	ABCF2	0,56
TMSB10	1,88	HSPD1	0,56
H2-AA	1,87	CXCL12	0,56
TNXB	1,86	INSC	0,57
SERPINA12	1,86	CRELD2	0,57
TNNC2	1,86	ETFDH	0,57
PCSK9	1,85	POLE4	0,57
ADAMTS2	1,85	SLC30A10	0,57
GCAP14	1,84	SBK	0,57
TUFT1	1,83	GNMT	0,57
OCIAD2	1,82		
SLC6A8	1,82		
KRT23	1,82		
ALS2CR4	1,82		
COL3A1	1,82		
D12ERTD647E	1,82		
FBLN1	1,82		
MFSD2	1,81		
SNCA	1,81		
H2-EB1	1,81		
KLK1B8	1,81		
FAM55B	1,81		
BC021614	1,81		
LTBP4	1,80		
GSTT2	1,80		
ENPP5	1,80		
PRSS8	1,79		

CRYGN	1,79		
MDK	1,79		
GABRB3	1,79		
CD63	1,79		
LPL	1,78		
LGALS8	1,78		
UBD	1,78		
NFE2	1,78		
CD74	1,78		
MB	1,78		
ADAMTSL2	1,78		
CAV1	1,77		
TTC3	1,77		
ARRDC3	1,77		
XLR4A	1,77		
MFAP4	1,77		
AKR1B3	1,76		
EMP1	1,76		
GOLM1	1,76		
TNNI2	1,76		
ESM1	1,75		
TTC39C	1,75		
INMT	1,75		
NID1	1,74		
IHH	1,74		
WT MCD vs WT chow			
gene name	fold up	gene name	Fold down
EIF2S3Y	24,34	CYP2B13	0,01
GSTA1	14,28	XIST	0,04
CYP4A12A	12,98	A1BG	0,05
CML4	12,16	CYP2B23	0,10
NUPR1	10,63	CYP2B9	0,10
SPINK3	9,11	FMO3	0,11
Mup21	8,58	HAO3	0,13
GPC1	7,26	BC014805	0,15
MMP12	6,67	ACOT1	0,16
GSTA2	6,25	FCER1G	0,18
CFD	5,93	CUX2	0,18
CYP4A12B	5,66	SERPINC1	0,20
CYP2D9	5,62	CTSC	0,22
FGF21	5,57	SULT3A1	0,22
ASNS	5,56	SERPINA1E	0,23
AQP4	5,43	SCNN1A	0,25
DDX3Y	5,01	CYP2C37	0,26
UHRF1	5,01	LARS2	0,27
PSAT1	4,85	NT5E	0,27
CIDEC	4,49	1700001C19RIK	0,28
GPNMB	4,39	DCT	0,28
ANXA2	4,17	MMD2	0,30
OLIG1	4,12	ACOT3	0,31
SRXN1	3,94	PIPOX	0,32
MCM6	3,90	ECI3	0,33
LY6D	3,86	TM7SF2	0,35
SCARA5	3,85	LRIT1	0,36
GSTP1	3,83	FABP5	0,37
UAP1L1	3,81	ST3GAL6	0,38
OSGIN1	3,70	CYP7A1	0,38
COX6A2	3,70	ZAP70	0,38

ADH7	3,69	PICALM	0,38
GM6484	3,62	CYP17A1	0,38
UBD	3,52	ES22	0,38
D17H6S56E-5	3,50	GSTT3	0,39
LPL	3,39	MBL2	0,40
HSD3B5	3,38	HACL1	0,40
MCM5	3,35	UGT2A3	0,41
LOC100048346	3,30	CYP2C29	0,41
NOX4	3,30	CES3B	0,41
FKBP11	3,22	EHHADH	0,41
LGALS3	3,21	CYP4A31	0,42
GM4956	3,19	GLB1	0,42
TFF3	3,13	RFX4	0,42
S100A11	3,13	CCL27	0,42
CCDC120	3,09	CPSF4L	0,42
SERPINA3K	3,07	CES1F	0,42
ARSA	3,04	CMTM8	0,42
KRT8	2,92	IGF1	0,43
TNFRSF12A	2,90	CYP4F14	0,43
PRC1	2,86	RGN	0,43
HAUS8	2,84	H2-BL	0,43
BEX2	2,82	NTRK2	0,43
UGT2B35	2,82	N4BP2L1	0,44
PRSS8	2,80	CYP2G1	0,44
SULT1E1	2,79	MACROD1	0,44
CXCL1	2,79	TMIE	0,44
MMP13	2,78	CES3	0,44
ALAS2	2,78	AFMID	0,45
USP18	2,76	AI317395	0,45
SMPD3	2,76	SDR42E1	0,45
CBR3	2,72	MT2	0,45
TREH	2,71	FAM55B	0,45
CDC20	2,71	CYP2C39	0,46
S3-12	2,68	PRLR	0,46
DNTT	2,68	ABCC6	0,46
TFRC	2,67	TLCD2	0,47
CXCL10	2,65	D0H4S114	0,47
C6	2,60	ABCA3	0,47
ATF3	2,59	G6PC	0,47
PVALB	2,58	HAMP2	0,47
APCS	2,58	GHR	0,47
SARS	2,57	RETSAT	0,47
NUDT18	2,55	SORL1	0,48
LCN2	2,55	2810410P22RIK	0,48
GSTM2	2,54	FAM25C	0,48
TES	2,52	SERPINA4-PS1	0,48
PBK	2,50	CYP3A11	0,48
JARID1D	2,48	ACAD10	0,49
AACS	2,48	ALDH3A2	0,49
CCL4	2,48	CYP2C67	0,49
TTC39A	2,44	SPATA2L	0,49
CLEC7A	2,44	RBKS	0,50
RSAD2	2,40	ACTB	0,50
ALDH1A1	2,37	SFRS5	0,50
TSKU	2,36	SCD1	0,50
PLEKHA1	2,35	PPM1K	0,50
TLR2	2,35	ABHD3	0,50
OMD	2,34	KLHL26	0,51
CKMT2	2,34	UAP1	0,51

CKM	2,31	DCLK3	0,51
TCAP	2,31	FAM123A	0,51
SPRR1A	2,29	ARL5A	0,51
IGFBP1	2,29	CSRP3	0,51
UNG	2,27	UGT3A1	0,51
GDF15	2,27	INCA1	0,51
KRT23	2,26	SLC27A5	0,51
CTSL	2,26	FGF1	0,52
TRIB3	2,26	SOCS2	0,52
BHLHB8	2,25	NOTUM	0,52
EIF4EBP1	2,24	ACOX1	0,52
PDK4	2,23	UGT1A2	0,52
TUBA8	2,22	CSTF3	0,52
LOC100047634	2,20	PEX19	0,52
NANS	2,19	SLC13A2	0,52
MAD2L1	2,18	HRSP12	0,52
ZFP330	2,17	RDH16	0,52
DUSP4	2,17	GNPDA1	0,52
RASSF3	2,16	BC024139	0,52
CDCA3	2,16	TMEM98	0,53
LOC100046163	2,16	TRFR2	0,53
TTN	2,16	LOC100046744	0,53
APOL9B	2,15	FAHD2A	0,53
CCND1	2,14	CCRN4L	0,53
TMC5	2,13	PRODH2	0,53
TUBB6	2,13	LOC100044087	0,53
LOC100038882	2,13	COLEC10	0,53
BIRC5	2,12	SLC11A2	0,53
CCNB1	2,10	CHRNA4	0,53
IGFBP2	2,10	FN3K	0,53
GMPPB	2,10	CFHR1	0,54
SRM	2,09	ZFP97	0,54
SCAMP5	2,08	ODZ3	0,54
1700067K01RIK	2,08	DUS4L	0,54
IRF7	2,08	SNTG2	0,54
CD63	2,08	DDO	0,54
PLK3	2,07	CCL25	0,54
AKR1B7	2,07	RCAN2	0,55
LOC626152	2,07	3010026O09RIK	0,55
TMEM86A	2,06	PLA1A	0,55
A230050P20RIK	2,06	AA415398	0,55
FEN1	2,06	SLC1A2	0,55
GMPPA	2,06	9030607L17RIK	0,55
MVP	2,05	PAQR9	0,55
CLN6	2,05	RTN4	0,56
MAT2A	2,05	MOSPD3	0,56
CYP2C55	2,05	ABCA6	0,56
CAP1	2,04	VLDLR	0,56
GADD45A	2,03	ACNAT2	0,56
E2F1	2,03	1810009N02RIK	0,56
CDC2A	2,03	SIAT7F	0,56
MLKL	2,02	F7	0,56
DUSP3	2,02	CRELD2	0,56
COX8B	2,02	PBLD	0,56
MCM2	2,01	ABCA8A	0,56
TREM2	2,00	ABHD1	0,56
SRPRB	2,00	PECR	0,56
MTHFD2	1,99	CRAT	0,56
ID1	1,99	FGL1	0,57

SETD8	1,99	CD163	0,57
FMN2	1,98	BACH2	0,57
S100A8	1,98	CLPX	0,57
SRPR	1,98	GCHFR	0,57
APOA5	1,97	DAPK1	0,57
IER3	1,97	1810049H13RIK	0,57
RPL3L	1,97	UCK1	0,57
DDIT3	1,97	NNMT	0,57
PDGFA	1,97	IGFALS	0,57
PGD	1,96	INMT	0,57
HIST1H2AN	1,95		
HIST1H2AD	1,95		
IFI202B	1,95		
TUBB2C	1,94		
ARSG	1,94		
PCSK9	1,94		
HTATIP2	1,94		
CHI3L3	1,93		
GET4	1,93		
EEF1A2	1,92		
EDEM2	1,92		
CHAF1A	1,92		
CXADR	1,92		
HIST1H2AF	1,92		
AREG	1,92		
CYP1A2	1,92		
FIGNL1	1,91		
IFI27	1,91		
AKR1C19	1,91		
LGMN	1,91		
H2-AB1	1,90		
SERPINA11	1,90		
GALE	1,89		
LOC100043257	1,89		
ANXA5	1,89		
SPATA24	1,89		
CAR3	1,89		
CYP7B1	1,89		
OASL1	1,88		
F2R	1,88		
HAPLN4	1,88		
IGTP	1,88		
ALDH1L2	1,88		
2700094K13RIK	1,88		
MIST1	1,87		
GSTA3	1,87		
MCM10	1,87		
NUSAP1	1,87		
TCEAL8	1,86		
S100A9	1,85		
GVIN1	1,85		
TNIP1	1,85		
CD68	1,84		
DYNLL1	1,84		
WBP5	1,83		
GM14492	1,83		
ANKRD56	1,83		
TUFT1	1,83		
CALML4	1,83		

ALDH1B1	1,83		
LY6A	1,83		
HIST1H2AK	1,82		
EIF6	1,82		
UNC13B	1,82		
STMN1	1,82		
RYR1	1,82		
ABCC12	1,82		
ALDH1A7	1,82		
BC048546	1,81		
TMEM97	1,81		
DBNDD2	1,81		
NECAB1	1,81		
PRKAG2	1,81		
GAS7	1,81		
IFI47	1,81		
GPR109A	1,81		
ARFGAP3	1,81		
NRM	1,80		
HR	1,80		
BTC	1,80		
ADAM32	1,80		
GSTP2	1,80		
CML2	1,80		
METTL1	1,80		
LIG1	1,80		
H2-EB1	1,79		
OTUD7B	1,79		
SUSD4	1,79		
VCL	1,79		
LOC100044439	1,79		
Ifi27l2b	1,79		
FMO5	1,79		
SLC39A7	1,78		
HIST1H4F	1,78		
OSBPL3	1,78		
SLAMF9	1,78		
GARS	1,77		
SEL1L3	1,77		
SLPI	1,77		
DBF4	1,77		
C9	1,77		
EAR4	1,77		
TMEM43	1,77		
LMNA	1,77		
AURKA	1,77		
PSMD8	1,77		
TNFRSF22	1,77		
TMEM176A	1,77		
OSTB	1,77		
APOA4	1,76		
SLC6A8	1,76		
GADD45B	1,76		
E130016E03RIK	1,76		
TMSB10	1,76		
BLNK	1,76		
TMEM184B	1,76		
HIST1H2AO	1,76		
HIST1H2AH	1,75		

LY6E	1,75		
CSTB	1,75		
JAM4	1,75		
SLC6A9	1,75		
LRH-1-/- MCD vs WT MCD			
gene name	fold up	gene name	Fold down
CYP2D12	41,45	HAMP2	0,07
TFF3	12,84	ALDH1B1	0,10
CYP2C29	6,70	APON	0,12
CORIN	6,50	MRAP	0,13
TINAG	5,54	ATP2A1	0,13
H2-BL	5,20	SERPINA3K	0,14
OLIG1	5,13	CYP2C39	0,19
NTRK2	5,04	OAT	0,19
PDE6C	4,61	PAQR9	0,20
EGR1	4,60	ACOT3	0,20
CYP2C55	4,57	CYP17A1	0,20
SPP1	4,25	GDF15	0,23
CYP4A12A	4,13	ANG	0,24
CYP2B9	4,03	NUPR1	0,28
FCER1G	3,60	UHRF1	0,28
SPINK3	3,56	MCM6	0,29
S3-12	3,44	OSGIN1	0,30
CES1	3,27	AI132487	0,30
BDH2	3,23	ARHGEF19	0,31
CYP7A1	3,16	GSTA1	0,32
SLPI	3,07	CYP8B1	0,32
PICALM	2,97	SPC25	0,32
FMO3	2,97	ORM2	0,32
BEX4	2,97	HGFAC	0,32
FAM55B	2,93	CFD	0,33
ABCB1B	2,91	DNTT	0,33
CYP2B23	2,88	FADS2	0,34
CYP2B10	2,81	PLK3	0,34
IHH	2,77	ABCG8	0,34
SFTPD	2,77	SULT1E1	0,34
EVC	2,75	VLDLR	0,35
AGXT2L1	2,69	FAM25C	0,35
TSPAN8	2,59	COX6A2	0,35
RBP1	2,58	ASNS	0,36
CTSC	2,53	PVALB	0,36
IGFBP5	2,52	LMNA	0,36
LARS2	2,51	SRXN1	0,36
SERPINA12	2,49	CYP4F14	0,36
AKR1B10	2,49	PRC1	0,36
CYP2G1	2,45	CCBL2	0,36
ESM1	2,43	SERPINA6	0,37
CYP2C50	2,42	RHBG	0,37
EVC2	2,41	AGPAT2	0,37
ESPN	2,41	FGF21	0,37
ACPL2	2,38	MCM5	0,37
ABCA3	2,36	APOL9B	0,37
AFM	2,36	SCD1	0,38
VIL1	2,36	TK1	0,38
NDRG1	2,34	ABCC3	0,38
TSC22D1	2,32	RNASE4	0,38
UPK3B	2,29	IGFBP1	0,38

AKR1C19	2,26	EXTL1	0,38
NUBP2	2,26	NUDT18	0,39
HSD17B2	2,25	RDH9	0,39
PPP1R14A	2,23	HSPB1	0,39
SNTA1	2,21	GDPD3	0,39
CRYM	2,20	THRSP	0,39
RANBP3L	2,19	D14ERTD449E	0,39
INMT	2,19	KRT75	0,39
TCEAL5	2,18	CDC20	0,40
STEAP2	2,17	SULT5A1	0,40
CYP2A5	2,15	TCAP	0,40
SERPINA4-PS1	2,15	GPNMB	0,41
H2-T10	2,14	MMD2	0,41
GABRB3	2,14	AKR1B7	0,41
AQP8	2,14	SDS	0,41
RAET1B	2,14	CKMT2	0,42
SNX15	2,13	RSAD2	0,42
MFGE8	2,12	CSAD	0,42
HSD17B6	2,11	ORM1	0,42
MBL2	2,11	TSKU	0,42
UAP1	2,11	LOC100047200	0,43
CEBPE	2,11	NT5E	0,43
BC014805	2,10	ANXA2	0,43
OMD	2,08	PBK	0,43
GM4956	2,07	NTN2L	0,43
UBD	2,06	TBX3	0,43
SQRDL	2,06	SAS	0,43
RDH16	2,04	LOC100047173	0,45
SUCNR1	2,04	GULO	0,45
GAS7	2,04	CAP1	0,45
NDUFB10	2,03	CDCA3	0,46
FOXQ1	2,03	TTN	0,46
CML4	2,03	ABCB4	0,46
CYP2B13	2,03	IGTP	0,46
CTGF	2,02	ABCG5	0,46
AXUD1	2,01	CCNB1	0,46
SLC27A1	2,00	GSTP1	0,46
NDRL	2,00	SCARB1	0,46
SLCO2A1	1,98	PSEN2	0,47
IFI27L2B	1,98	CKM	0,47
FMN2	1,97	PSMD8	0,47
GPX6	1,96	PKLR	0,47
STK39	1,94	LITAF	0,47
CYP3A11	1,93	GNAT1	0,47
IDI1	1,93	PPL	0,48
C9	1,92	DHCR24	0,48
EPDR1	1,92	CBR3	0,48
SULT1C2	1,89	PAOX	0,48
MUP20	1,89	DUSP6	0,48
MUP5	1,88	BIRC5	0,49
RNASE1	1,88	MMP12	0,49
ACNAT2	1,87	POR	0,49
OLFM3	1,85	PDE6H	0,49
1810011O10RIK	1,84	GPT2	0,49
ARL5A	1,83	ABCC2	0,49
HIST1H4K	1,83	CIB2	0,50
5033411D12RIK	1,82	LOC100047579	0,50
H2-AA	1,82	CCND1	0,50
BICC1	1,82	IL1RN	0,50

IRF6	1,82	TSPAN31	0,50
CRYL1	1,81	ANG2	0,50
LY6E	1,80	HIST1H2AD	0,50
AKR1B3	1,78	CTH	0,51
PER1	1,76	GBP3	0,51
GHR	1,76	LOC100047762	0,51
ACAD12	1,76	GNMT	0,51
TOB2	1,76	FMO5	0,51
PRR18	1,75	HES6	0,51
GAL3ST1	1,75	APOA4	0,52
AOX3	1,75	AGPAT9	0,52
CRYGN	1,74	PARP16	0,52
		BCL2L11	0,52
		ITPR2	0,52
		CYP3A25	0,52
		TIAM2	0,52
		ST6GAL1	0,53
		FIGNL1	0,53
		CDC2A	0,53
		HIST1H2AN	0,53
		CBR1	0,53
		NAGS	0,53
		SERPINA1E	0,53
		MCM2	0,53
		PNPLA7	0,53
		HIST1H2AF	0,53
		GADD45A	0,53
		LOC677317	0,53
		ELOVL6	0,54
		MOD1	0,54
		OSTB	0,54
		BCMO1	0,54
		ITIH3	0,54
		ABCD1	0,54
		1700019G17RIK	0,54
		CAMK1D	0,54
		HR	0,54
		HIST1H2AO	0,54
		ATF3	0,54
		COX8B	0,54
		UNC13B	0,54
		EEF1A2	0,54
		RCAN2	0,55
		GLS2	0,55
		PSAT1	0,55
		OAF	0,55
		AQP11	0,55
		AFMID	0,55
		GSTM2	0,55
		HSPB8	0,55
		DUSP4	0,55
		HDC	0,56
		SEC14L4	0,56
		RAD54B	0,56
		TMTC2	0,56
		ELOVL5	0,56
		TTC39A	0,56
		TRIB3	0,56
		RPL3L	0,56

		CML2	0,57
		SLC16A10	0,57
		INHBE	0,57